# Phosphatidic Acid Mediates the Nem1-Spo7/Pah1 Phosphatase Cascade in Yeast Lipid Synthesis

Joanna M. Kwiatek[1] , Bryan Gutierrez[1,2] , Enver Cagri Izgu[1,2,3] , Gil-Soo Han[1,4] , and George M. Carman[1,4]*

[1]Rutgers Center for Lipid Research, New Jersey Institute for Food, Nutrition, and Health, Rutgers University, New Brunswick, New Jersey, USA, [2]Department of Chemistry and Chemical Biology, Rutgers University, New Brunswick, New Jersey, USA, [3]Cancer Institute of New Jersey, Rutgers University, New Brunswick, New Jersey, USA, and [4]Department of Food Science, Rutgers University, New Brunswick, New Jersey, USA

Abstract In the yeast *Saccharomyces cerevisiae*, the *PAH1*-encoded Mg^{2+}-dependent phosphatidate (PA) phosphatase Pah1 regulates the bifurcation of PA to diacylglycerol (DAG) for triacylglycerol (TAG) synthesis and to CDP-DAG for phospholipid synthesis. Pah1 function is mainly regulated via control of its cellular location by phosphorylation and dephosphorylation. Pah1 phosphorylated by multiple protein kinases is sequestered in the cytosol apart from its substrate PA in the membrane. The phosphorylated Pah1 is then recruited and dephosphorylated by the protein phosphatase complex Nem1 (catalytic subunit)-Spo7 (regulatory subunit) in the endoplasmic reticulum. The dephosphorylated Pah1 hops onto and scoots along the membrane to recognize PA for its dephosphorylation to DAG. Here, we developed a proteoliposome model system that mimics the Nem1-Spo7/Pah1 phosphatase cascade to provide a tool for studying Pah1 regulation. Purified Nem1-Spo7 was reconstituted into phospholipid vesicles prepared in accordance with the phospholipid composition of the nuclear/endoplasmic reticulum membrane. The Nem1-Spo7 phosphatase reconstituted in the proteoliposomes, which were measured 60 nm in an average diameter, was catalytically active on Pah1 phosphorylated by Pho85-Pho80, and its active site was located at the external side of the phospholipid bilayer. Moreover, we determined that PA stimulated the Nem1-Spo7 activity, and the regulatory effect was governed by the nature of the phosphate headgroup but not by the fatty acyl moiety of PA. ⓙ The reconstitution system for the Nem1-Spo7/Pah1 phosphatase cascade, which starts with the phosphorylation of Pah1 by Pho85-Pho80 and ends with the production of DAG, is a significant advance to understand a regulatory cascade in yeast lipid synthesis.

Supplementary key words phosphatidate • diacylglycerol • triacylglycerol • phosphatidate phosphatase • Pho85-Pho80 • Nem1-Spo7 protein phosphatase • endoplasmic reticulum • phospholipid bilayer • reconstitution • proteoliposome
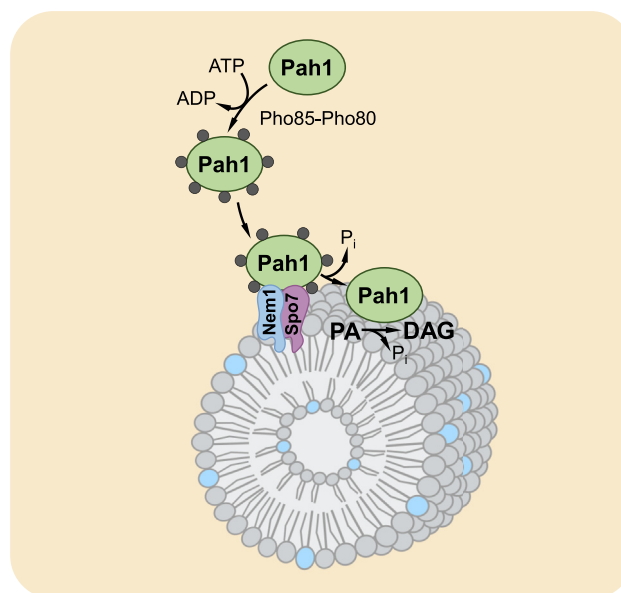
In the budding yeast *Saccharomyces cerevisiae*, the major phospholipids of the nuclear/ER membrane include phosphatidylcholine (PC), phosphatidylethanolamine (PE), phosphatidylinositol (PI), and phosphatidylserine (PS) (1, 2). In the primary de novo pathway (**Fig. 1**), these phospholipids are derived from the branch point intermediate phosphatidate (PA), which itself is synthesized in the nuclear/ER membrane (6–12). The PA is activated with CTP to form another branch point intermediate, the liponucleotide CDP-diacylglycerol (DAG) (13, 14). In the nuclear/ER membrane, CDP-DAG donates its phosphatidyl moiety to inositol to form PI (15–17) or to serine to form PS (18–21). The PS synthesized in the nuclear/ER is transported to the mitochondrial membrane (22, 23) and decarboxylated to form PE (24, 25), which is then transported to the nuclear/ER membrane and subjected to three successive steps of methylation to form PC (26–29). The
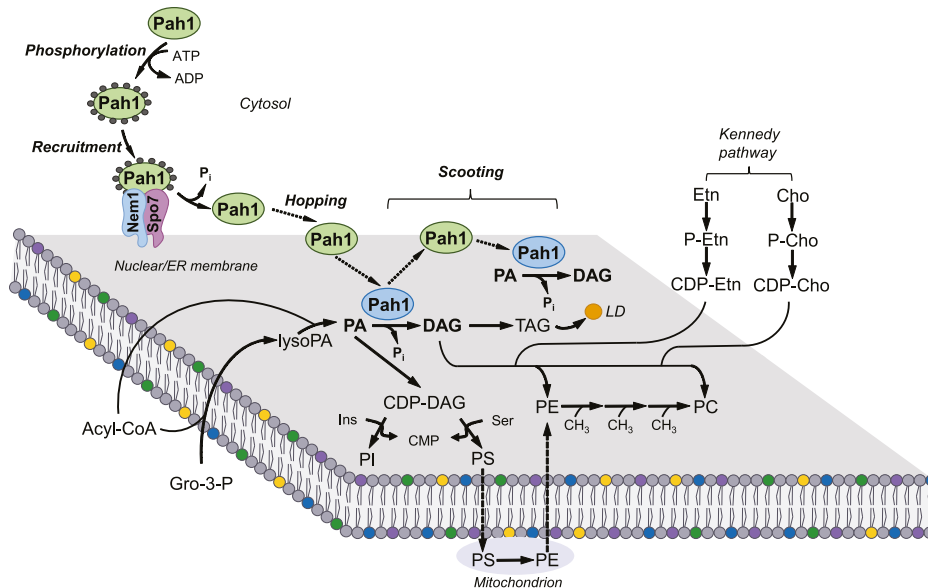
Fig. 1. Model for the phosphorylation/dephosphorylation-mediated regulation of Pah1 PAP location and mode of action of the enzyme at the nuclear/ER membrane via the hopping and scooting modes. Pah1 in the cytosol is phosphorylated by several protein kinases. The phosphorylated enzyme (*gray circles*) translocates to the nuclear/ER membrane via its recruitment and dephosphorylation by the Nem1-Spo7 protein phosphatase complex. Dephosphorylated Pah1 hops onto the membrane, scoots along the surface to bind its substrate, and catalyzes the dephosphorylated PA to produce DAG, which can be utilized in the formation of TAG stored in lipid droplets (LDs). Following the PAP reaction, Pah1 scoots along the membrane until it recognizes a PA molecule for another round of reaction. Pah1 catalyzing the PAP reaction is designated with blue color. PA is also converted to CDP-DAG for the synthesis of the membrane phospholipids PI, PS, phosphatidylethanolamine (PE), and PC. The phospholipids PE and PC may also be derived from DAG via the CDP-ethanolamine and CDP-choline branches of the Kennedy pathway when cells are supplemented with ethanolamine and/or choline. Further details of the lipid synthesis pathways may be found elsewhere (3–5). PA, phosphatidate; PAP, phosphatidate phosphatase; PC, phosphatidylcholine; PI, phosphatidylinositol; PS, phosphatidylserine.

synthesis of these phospholipids primarily occurs when cells are actively growing (e.g., exponential phase) and need to make cellular membranes, but as cells progress into stasis (e.g., stationary phase), the intermediate PA is primarily channeled into the storage lipid tri-acylglycerol (TAG) via DAG (30, 31). The TAG produced in this pathway is then stored in cytoplasmic lipid droplets (32, 33). The DAG produced from PA (34, 35) may also be used by ethanolamine and/or choline auxotrophic mutants (27–29, 36–40) defective in CDP-DAG-dependent synthesis of PS, PE, and/or PC by way of the CDP-ethanolamine (41–44) and/or CDP-choline (45–48) branches of the Kennedy pathway. Of note, phospholipids and TAG, as well as lipid droplets, may be produced at the inner nuclear membrane in genetically modified cells (49).

The bifurcation of PA between CDP-DAG and DAG is a crucial point in lipid synthesis regulation, and among the enzymes that utilize PA at this branch point, the *PAH1*-encoded Mg^{2+}-dependent PA phosphatase (PAP) (also known as Pah1) (35) has emerged as a key regulator of PA consumption (2, 50–54). In fact, disturbances in the bifurcation of PA as mediated by Pah1 give rise to a variety of lipid-based abnormalities (e.g., nuclear/ER membrane expansion, lipodystrophy, and fatty acid-induced lipotoxicity) and defects in cellular physiology that lead to apoptosis and reduction in chronological life span (2–4, 55). Thus, knowledge of

Pah1 regulation is of fundamental importance. It is known that Pah1 is regulated by genetic and biochemical mechanisms (2, 51–54, 56). Pah1 expression is regulated by growth phase and nutrient status; increased expression as mediated by nutrient depletion in stationary phase is coincident with PA utilization for TAG synthesis, whereas reduced expression as mediated by nutrient sufficiency in exponential phase is coincident with PA utilization for phospholipid synthesis (31, 57). The PAP activity of Pah1 is modulated by lipids (58, 59), nucleotides (60), and the phosphorylation status (61–70). For example, PAP activity is stimulated by CDP-DAG and PI (58), whereas the enzyme activity is inhibited by sphingoid bases (59) and the nucleotides ATP and CTP (60). Multiple protein kinases phosphorylate Pah1 (63–69), whereas the phosphorylated enzyme is dephosphorylated by the Nem1 (catalytic subunit)-Spo7 (regulatory subunit) phosphatase complex (61, 70, 71). Whereas some of its phosphorylations (e.g., by Pho85-Pho80 and Rim11) inhibit PAP activity (64, 69), the dephosphorylation by Nem1-Spo7 stimulates activity (64, 70). Pah1 phosphorylation and dephosphorylation, respectively, are generally associated with reduced and elevated enzyme function (54).

The most important factor responsible for Pah1 function is its cellular location, which is controlled by its phosphorylation and dephosphorylation (54) (Fig. 1). After its expression, Pah1 in the cytosol is

phosphorylated by multiple protein kinases (54). The phosphorylation stabilizes the enzyme (72) but makes it nonfunctional because it is sequestered in the cytosol apart from its substrate PA that resides in the nuclear/ER membrane. Phosphorylated Pah1 translocates to the nuclear/ER membrane through its recruitment and dephosphorylation by the Nem1-Spo7 protein phosphatase complex (61–65, 71, 73–76). Dephosphorylated Pah1 hops onto the membrane via its N-terminal amphipathic helix (73), scoots along the surface to recognize its substrate PA, and catalyzes the dephosphorylated PA to produce DAG (77). Following the PAP reaction, Pah1 scoots along the membrane for another round of reaction (77).

The aim of this work is to develop a proteoliposome model system that mimics the Nem1-Spo7/Pah1 phosphatase cascade that occurs at the nuclear/ER membrane. In a previous study, we showed that a liposome composed of PC, PE, PI, PS, and PA, which mimics the phospholipid composition of the nuclear/ER membrane (1, 78, 79), provides a suitable model for the action of unphosphorylated Pah1 to hop and scoot along the membrane surface and catalyze the PAP reaction (77). Herein, we significantly advanced this in vitro model for studying the dephosphorylation of Pah1 at the membrane surface by the Nem1-Spo7 complex reconstituted in the PC/PE/PI/PS/PA liposomes. We discovered that the PAP substrate PA stimulates the Nem1-Spo7 complex-mediated dephosphorylation of Pah1 and demonstrated that the Nem1-Spo7/Pah1 phosphatase cascade, starting with the phosphorylation of Pah1 and ending with the generation of DAG from PA, was reconstituted in the Nem1-Spo7 proteoliposome system.

MATERIALS AND METHODS

Materials

Avanti Polar Lipids and Analtech were the sources of lipids and silica gel GHL TLC plates, respectively. Bio-Rad was the source of molecular mass protein standards and reagents for protein assay, SDS-PAGE, and Western blotting. InstantBlue protein stain was from Expedeon. GE Healthcare was the source of the enhanced chemifluorescence Western blotting detection kit, Sephadex G-50 superfine, IgG-Sepharose, Q-Sepharose, and polyvinylidene difluoride paper. MilliporeSigma was the source of ammonium molybdate, bovine serum albumin, Triton X-100, and rabbit anti-protein A antibody (product P3775, lot 025K4777). PerkinElmer Life Sciences and National Diagnostics, respectively, were the sources of radiochemicals and scintillation-counting supplies. Thermo Fisher Scientific was the source of malachite green, alkaline phosphatase-conjugated goat anti-rabbit IgG antibody (product no. 31340, lot number: NJ178812), and Pierce strong anion exchange spin columns and protein concentrators 30K. Qiagen was the source of nickel-nitrilotriacetic acid-agarose resin. Anti-Spo7 antibody was previously produced in New Zealand White rabbits (80). Wako Chemicals supplied Phos-tag™ Acrylamide AAL-107. All other chemicals were reagent grade.

Purification of enzymes

The strains and plasmids used for the purification of enzymes are listed in Table 1. Protein A-tagged Nem1-Spo7 protein phosphatase complex was purified from *S. cerevisiae* strain RS453-expressing plasmids YCplac111-*GAL1/10-NEM1*-PtA and pRS313-*GAL1/10-SPO7* by affinity chromatography with IgG-Sepharose (85) with minor modifications (70). His$_6$-tagged Pah1 and Pah1-D398E expressed from plasmids pGH313 and pGH313-D398E, respectively, in *Escherichia coli* strain BL21(DE3)pLysS were purified by affinity chromatography with nickel-nitrilotriacetic acid-agarose (35), followed by ion exchange chromatography with Q-Sepharose (70). Tandem affinity purification-tagged Pah1 expressed from plasmid pGH452 in *S. cerevisiae* strain SS1132 was purified by affinity chromatography with IgG-Sepharose, followed by anion exchange chromatography and size-exclusion chromatography (86). His$_6$-tagged Pho85-Pho80 protein kinase complex was purified from *E. coli* strain BL21(DE3)-expressing plasmids EB1164 and EB1076 by affinity chromatography with nickel-nitrilotriacetic acid-agarose (84). The purified enzyme preparations were analyzed by SDS-PAGE and judged to be highly purified; the enzymes were stored at −80°C.

Preparation of Nem1-Spo7 proteoliposomes

Nem1-Spo7 proteoliposomes were prepared by the size-exclusion chromatography as described by Mimms *et al.* (87) with minor modifications (88–90). Unless otherwise indicated, the dioleoyl derivatives of PC, PE, PS, PA, and soybean PI were used in this work. Under most conditions used in this study,

TABLE 1. Strains and plasmids used in this study

Strain or Plasmid	Genotype or Relevant Characteristics	Source or Reference
Strain		
Saccharomyces cerevisiae		
RS453	*MAT**a** ade2-1 his3-11,15 leu2-3,112 trp1-1 ura3-52*	(81)
SS1026	*pah1Δ::TRP1* derivative of RS453	(61)
Escherichia coli		
BL21(DE3)pLysS	F⁻ *ompT hsdS$_B$ (r$_B^-$ m$_B^-$) gal dcm* (DE3) pLysS	Novagen
BL21(DE3)	F⁻ *ompT hsdS$_B$ (r$_B^-$ m$_B^-$) gal dcm* (DE3)	Invitrogen
Plasmid		
YCplac111-*GAL1/10-NEM1*-PtA	*NEM1*-PtA under control of *GAL1/10* promoter inserted in *CEN/LEU2* plasmid	(61)
pRS313-*GAL1/10-SPO7*	*SPO7* under control of *GAL1/10* promoter inserted in *CEN/HIS3* plasmid	(82)
pGH313	*PAH1* coding sequence inserted into pET-15b	(35)
pGH313-D398E	pGH313 containing the D398E mutation in the *PAH1* coding sequence	(83)
EB1164	*PHO85*-His$_6$ derivative of pQE-60	(84)
EB1076	*PHO80* derivative of Psbeta	(84)

the phospholipid composition of liposomes was PC/PE/PI/PS/PA (33.75:22.5:22.5:11.25:10 mol %). Additional liposomes were made of PC/PE/PI/PS (37.5:25:25:12.5 mol %), PC/PE/PI/PS/ThioPA (33.75:22.5:22.5:11.25:10 mol %), and PC/PE/PI/PS/DAG (33.75:22.5:22.5:11.25:10 mol %). The mol % of PA in the liposome composed of PC/PE/PI/PS/PA was calculated using the following formula, mol $\%_{PA}$ = (PA [molar])/(PA [molar] + PC [molar] + PE [molar] + PI [molar] + PS [molar]) × 100. Briefly, chloroform was evaporated from phospholipid mixtures under a stream of nitrogen to form a thin film, and residual solvent was removed in vacuo. Phospholipids were resuspended in 280 mM octyl glucoside to a final phospholipid concentration of 20 mM. The octyl glucoside/phospholipid-mixed micelles were then mixed with 9 μg of Nem1-Spo7 complex solubilized in 1.7 mM Triton X-100. The final molar ratios of octyl glucoside to Triton X-100 and octyl glucoside to phospholipids were 164:1 and 14:1, respectively. The reconstitution mixture (137 μl) was applied to and eluted from a Sephadex G-50 superfine column (1 × 4 cm) equilibrated at 4°C with a chromatography buffer consisting of 25 mM Tris-HCl (pH 8.0), 250 mM NaCl, and 10 mM 2-mercaptoethanol at 4°C. The presence of phospholipids and the Nem1-Spo7 complex, respectively, in the column fractions was analyzed by primuline staining of lipid spots on a TLC plate and Western blotting with anti-protein A and anti-Spo7 antibodies. Relative amounts were determined by fluorimaging; the image intensities were quantified with ImageJ software. The size of the proteoliposomes in the peak fraction, which we used in these studies, was determined by light scattering using a Brookhaven Instruments Particle Size Analyzer. Proteoliposomes were stored for no longer than one week at 4°C.

Lipid analysis of Nem1-Spo7 proteoliposomes

Lipids were extracted from proteoliposomes by the method of Bligh and Dyer (91). Phospholipids and DAG, respectively, were resolved by one-dimensional TLC on silica gel plates using the solvent systems chloroform/ethanol/water/triethylamine (30:35:7:35, v/v) (92) and hexane/diethyl ether/glacial acetic acid (40:10:1, v/v) (93). The resolved lipids were stained with 0.5% primuline. The amounts of PA and DAG in the proteoliposomes were determined from standard curves of each lipid on TLC plates. Fluorimaging using a Storm 860 Molecular Imager (GE Healthcare) was used to acquire fluorescence signals from the plates; the intensities of the images were analyzed by ImageJ software. The identity of the lipids was confirmed by comparison with the migration of authentic standards.

Nem1-Spo7 protein phosphatase assay

Nem1-Spo7 phosphatase activity was measured at 30°C by following an increase in electrophoretic mobility of Pah1 in SDS-PAGE (70, 94) or by following the release of $^{32}P_i$ from [^{32}P]Pah1 (200-1,400 cpm/nmol) (70). The reaction mixture contained 100 mM sodium acetate (pH 5.0), 10 mM MgCl$_2$, 1 mM DTT, 0.2 μM phosphorylated Pah1, and Nem1-Spo7 proteoliposomes in a total volume of 20 μl. In the nonradioactive assay, the reaction was terminated with Laemmli sample buffer (95) followed by SDS-PAGE in the absence and presence of the Phos-tag reagent (70, 94). In the radioactive assay, the reaction was terminated by the addition of 20% trichloroacetic acid and 0.4 mg/ml bovine serum albumin. The mixture was cooled on ice for 15 min and then centrifuged for 20 min at 15,000 g to precipitate the radioactive

substrate. The supernatant containing $^{32}P_i$ was measured for radioactivity by scintillation counting. One unit of Nem1-Spo7 phosphatase activity was defined as the amount of enzyme that catalyzed the formation of 1 nmol phosphate per min. The Nem1-Spo7 phosphatase reactions, which were conducted in triplicate at 30°C, were linear with time and protein concentration. To prepare [^{32}P]Pah1, E. coli-expressed unphosphorylated Pah1 was phosphorylated by the Pho85-Pho80 protein kinase complex using 100 μM [γ-^{32}P]ATP (5,000–10,000 cpm/pmol) as described previously (64). [^{32}P]Pah1 was purified by Q-Sepharose chromatography to remove the Pho85-Pho80 protein kinase (70).

PAP assay

PAP activity was measured at 30°C for 15 min by following the release of water-soluble P$_i$ from chloroform-soluble PA; the P$_i$ produced in the reaction was measured with malachite green-molybdate reagent (96, 97). The reaction mixture contained 50 mM Tris-HCl (pH 7.5), 1 mM MgCl$_2$, enzyme protein, and the PA-containing liposomes (77) in a final volume of 10 μl. Enzyme assays were conducted in triplicate, and the average SD of the assays was ± 5%. All enzyme reactions were linear with time and protein concentration. One unit of enzymatic activity was defined as the amount of enzyme that catalyzed the formation of 1 nmol of product per minute.

SDS-PAGE and Western blotting

SDS-PAGE (95) and Western blotting (98, 99) with polyvinylidene difluoride membrane were performed by standard procedures. Phos-tag™ AAL-107 (20 μM) and MnCl$_2$ (100 μM) were added to 5% polyacrylamide gels for analysis of the phosphorylation state of Pah1. The samples for Western blotting were normalized to total protein loading. The membrane was cut and the upper and lower portions, respectively, were probed with rabbit anti-protein A (2 μg/ml) and rabbit anti-Spo7 (1 μg/ml) antibodies. The goat anti-rabbit IgG antibody conjugated with alkaline phosphatase was used at a dilution of 1:4,000. Immune complexes were assayed with the enhanced chemifluorescence Western blotting substrate. Fluorescence signals from the blots were visualized by fluorimaging with a Storm 865 Molecular Imager (GE Healthcare) and image intensities were analyzed with ImageJ software.

Preparation of ThioPA

ThioPA (C18:1) was synthesized as described by Bonnel et al. (100) with some modifications. Details on the synthesis and characterization of this phospholipid are found in the Supporting information.

Data analysis

Microsoft Excel software was used for the statistical analysis of the data; the P values < 0.05 were taken as a significant difference. SigmaPlot software was used to analyze kinetic data.

RESULTS

Reconstitution of the Nem1-Spo7 protein phosphatase complex into phospholipid vesicles

We sought to reconstitute the Nem1-Spo7 phosphatase complex into PC/PE/PI/PS/PA vesicles to mimic

the in vivo environment of the complex in the nuclear/ ER membrane (1, 78, 79) to recruit and dephosphorylate Pah1 (61, 62, 70, 71, 73). It has been shown that Pah1 PAP activity on PA in this phospholipid composition is higher than the enzyme activity on simple PC/PA phospholipid vesicles or Triton X-100/PA-mixed micelles (77). For the preparation of the Nem1-Spo7 proteoliposomes, we utilized the chromatographic method of Mimms *et al.* (87) that had been applied to the reconstitution of the membrane-associated phospholipid biosynthetic enzymes glycerol-3-phosphate acyltransferase (88), PI synthase (89), and PS synthase (90) into unilamellar phospholipid vesicles. Triton X-100/ Nem1-Spo7 complex micelles (70, 71) were mixed with octyl glucoside/phospholipid micelles and fractionated by size-exclusion chromatography with Sephadex G-50 superfine. As expected (87–90), the Nem1-Spo7 proteoliposomes were eluted from the column near the void volume, and the peak fractions of phospholipids, Nem1, and Spo7 were coincident (Fig. 2A). The TLC analysis of the proteoliposomes confirmed that the vesicles were composed of PC, PE, PI, PS, and PA (Fig. 2A, *right*), and the relative amounts of the phospholipids were estimated from their input amounts. The peak fractions of Triton X-100 and octyl glucoside micelles, which are well separated from the proteoliposomes, were contained in the later elution fractions that are not shown in Fig. 2A (87–90). Light scattering analysis of the Nem1-Spo7 proteoliposomes in the peak fractions, which were used in these studies, indicated the average diameter of 60 nm (Fig. 2B), a value within the range of vesicle sizes (40–90 nm) of reconstituted glycerol-3-phosphate acyltransferase, PI synthase, and PS synthase (88–90). Disruption of the proteoliposomes with Triton X-100 did not result in a significant increase in Nem1-Spo7 phosphatase activity, indicating that the phosphatase complex is asymmetrically reconstituted with its active site located outside of the vesicle. Proteoliposomes stored at 4°C maintained Nem1-Spo7 phosphatase activity for at least one week.

Nem1-Spo7 proteoliposomes catalyze the dephosphorylation of Pah1

The fidelity of the Nem1-Spo7 proteoliposomes to catalyze the dephosphorylation of Pah1 was examined by two different assays. In the first assay, the protein phosphatase activity was measured by following a change in the electrophoretic mobility of Pah1 in SDS-PAGE (70, 94, 101). In the second assay, the enzyme activity was measured by following the release of $^{32}P_i$ from ^{32}P-labeled Pah1 (70). As a substrate of Nem1-Spo7, two forms of phosphorylated Pah1 were used in this study: 1) Pah1 prepared from yeast (62, 102–114), which is endogenously phosphorylated by multiple protein kinases and 2) (63–68) Pah1 heterologously expressed in *E. coli* and phosphorylated in vitro by the Pho85-Pho80 protein kinase (64). Pho85-Pho80, which phosphorylates seven sites on Pah1, has strong
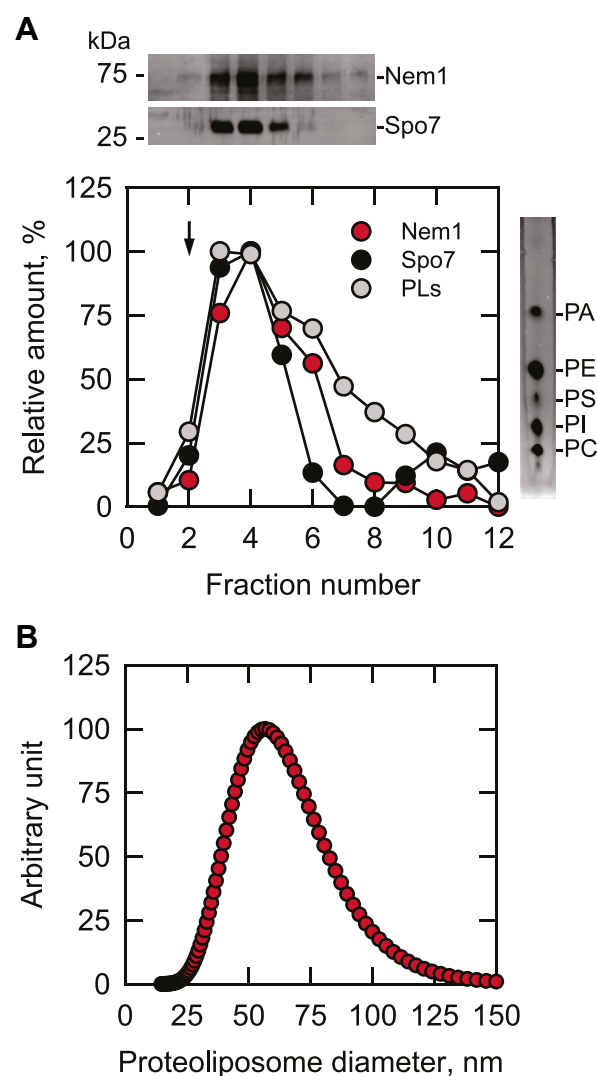

Fig. 2. Preparation and analysis of Nem1-Spo7 proteoliposomes. A: octyl glucoside/phospholipid micelles were mixed with Triton X-100/Nem1-Spo7 complex micelles, followed by size-exclusion chromatography with Sephadex G-50 superfine. The elution fractions (0.5 ml) were analyzed for Nem1 and Spo7 by Western blotting (*upper*) with anti-protein A and anti-Spo7 antibodies, respectively, and for total phospholipids (PLs) by TLC and primuline staining (*right*). The amounts of Nem1, Spo7, and phospholipids were quantified by ImageJ software; the amount of each component in the peak fraction was set at 100%. The phospholipid composition of the peak fraction was analyzed by TLC; the positions of the individual phospholipids are indicated (*right*). The *arrow* in the figure indicates the position of the void volume. B: the peak fraction of Nem1-Spo7 proteoliposomes was subjected to particle size measurement by light scattering.

regulatory effects on the protein location, stability, and PAP activity (54, 62–64, 70, 72).

In the electrophoretic mobility shift assay, the reconstituted Nem1-Spo7 catalyzed the time-dependent dephosphorylation of Pah1 phosphorylated in vivo (Fig. 3A) and in vitro (Fig. 3B) as indicated by an increase in the mobility of the protein. To better distinguish the phosphorylated and dephosphorylated forms
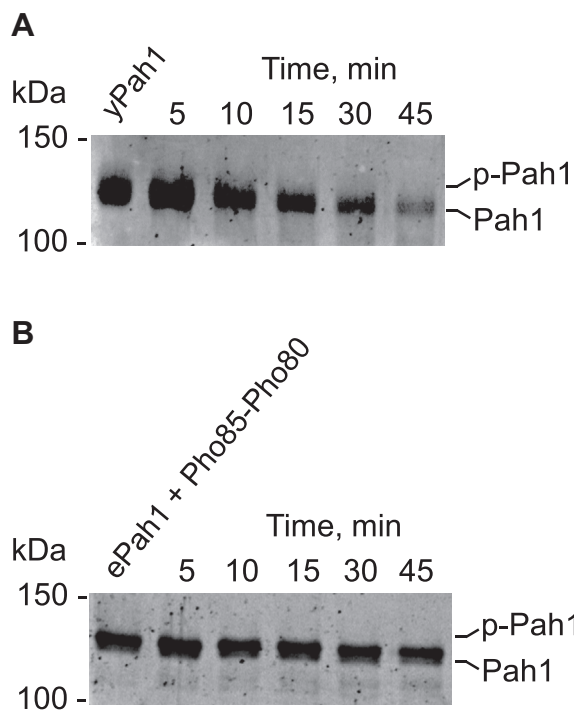
A

B

Fig. 3. Nem1-Spo7 proteoliposomes catalyze the time-dependent dephosphorylation of Pah1. Nem1-Spo7 proteoliposomes were incubated for the indicated time periods with purified Pah1 endogenously phosphorylated in yeast (*yPah1*) (A) or *Escherichia coli*-expressed and purified Pah1 phosphorylated by Pho85-Pho80 (*ePah1 + Pho85-Pho80*) (B). Following the incubations, the samples were subjected to SDS-PAGE using a 5% polyacrylamide gel followed by staining with Coomassie blue. The positions of phosphorylated (*p-Pah1*) and dephosphorylated Pah1 and molecular mass standards are indicated. The data shown is representative of three separate experiments.

of Pah1, we examined its mobility in the polyacrylamide gel containing the Phos-tag reagent, which traps phosphorylated proteins (115) and retards their electrophoretic mobility (70, 101) (**Fig. 4**A). Using the Phos-tag polyacrylamide gel, we could more readily discern changes in electrophoretic mobility and showed that the dephosphorylation of endogenously phosphorylated Pah1 (Fig. 4B) and Pah1 phosphorylated by Pho85-Pho80 in vitro (Fig. 4C) is dependent on the amount of the Nem1-Spo7 proteoliposomes. In addition, the dephosphorylation of Pah1 resulted in its degradation as reflected by the reduction of protein abundance (Fig. 4B, C).

In the radioactive assay for Nem1-Spo7 activity, which is more sensitive and quantitative, a ^{32}P-labeled substrate was prepared by phosphorylating the *E. coli*-expressed unphosphorylated Pah1 by Pho85-Pho80 with [γ-^{32}P]ATP. The amount of $^{32}P_i$ released from [^{32}P]Pah1 by Nem1-Spo7 was measured by scintillation counting after the removal of both phosphorylated and dephosphorylated forms of the protein by trichloroacetic acid precipitation (70). The Nem1-Spo7 phosphatase activity was linear over a 10-min incubation period and dependent on the concentration of phosphorylated Pah1 (**Fig. 5**). The radioactive assay was not performed on
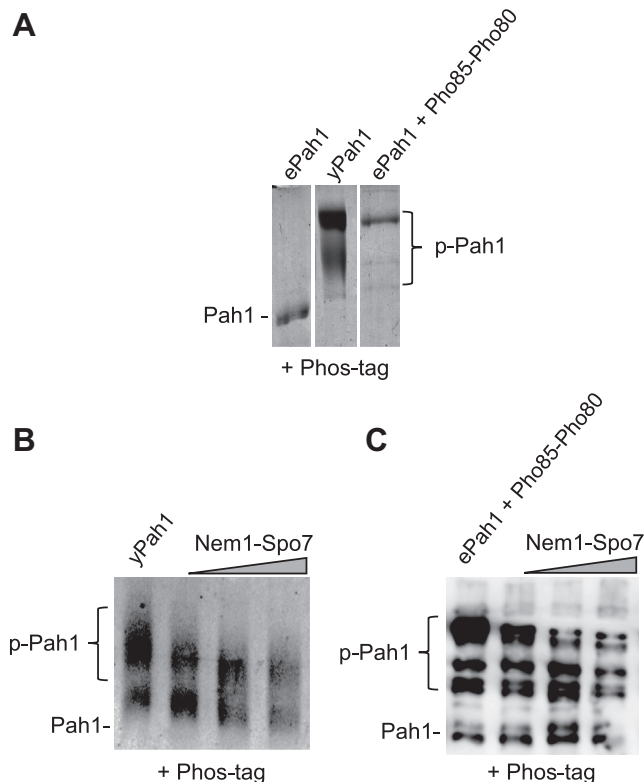
A

B

C

Fig. 4. Pah1 dephosphorylation is dependent on the amount of Nem1-Spo7 proteoliposomes. Purified Pah1 endogenously phosphorylated in yeast (*yPah1*) (A, B), Pah1 expressed and purified from *Escherichia coli* (*ePah1*) (A), and *E. coli*-expressed and purified Pah1 phosphorylated by Pho85-Pho80 (*ePah1 + Pho85-Pho80*) (A, C) were subjected to SDS-PAGE using a 6% polyacrylamide gel containing 20 μM Phos-tag and 100 μM MnCl₂. The phosphorylated forms of Pah1 (B, C) were incubated for 45 min with increasing amounts of Nem1-Spo7 proteoliposomes. The resolved proteins were stained with Coomassie blue. The positions of phosphorylated (*p-Pah1*) and dephosphorylated forms of Pah1 are indicated. The data shown is representative of three separate experiments.

endogenously phosphorylated Pah1 owing to the cumbersome nature of purifying radiolabeled Pah1 from yeast cells. Overall, Nem1-Spo7 phosphatase activity in the proteoliposome system was dependent on time, the amount of the phosphatase complex, and the concentration of phosphorylated Pah1. The dephosphorylation of Pah1 was not observed when the phosphatase reaction was performed with liposomes without the reconstituted Nem1-Spo7 complex.

PA stimulates Nem1-Spo7 phosphatase activity

The Nem1-Spo7 proteoliposomes contained PA because it is a component of the nuclear/ER membrane (1, 78, 79) and the substrate for the PAP reaction (34). The PA concentration in the nuclear/ER membrane is largely controlled by Pah1 PAP activity (33, 35), and thus, we considered whether the PA concentration affects the Nem1-Spo7 activity on Pah1. To address this question, Pah1 phosphorylated by Pho85-Pho80 was incubated with Nem1-Spo7 proteoliposomes prepared
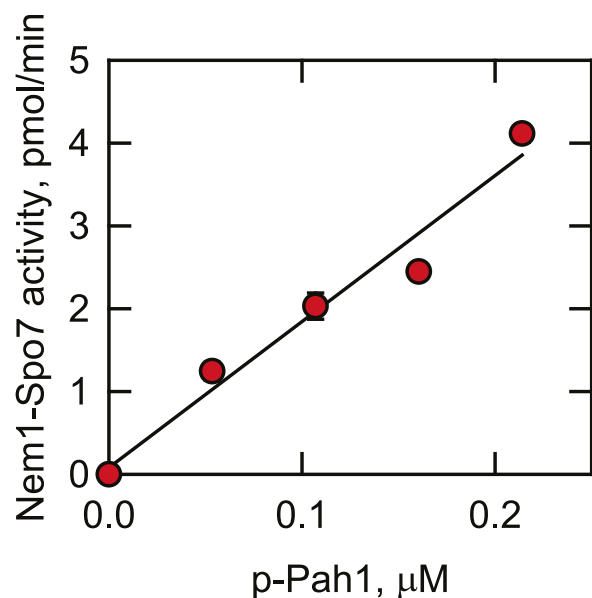
Fig. 5. The protein phosphatase activity of Nem1-Spo7 proteoliposomes is dependent on the concentration of phosphorylated Pah1. *Escherichia coli*-expressed and purified unphosphorylated Pah1 was phosphorylated by Pho85-Pho80 with [γ-^{32}P]ATP. The Nem1-Spo7 protein phosphatase activity was measured for 10 min by following the release of ^{32}P$_i$ from the indicated concentrations of [^{32}P]Pah1. The data shown in the figure is the average of three independent experiments ± S.D. (*error bars*). The error bars are hidden behind some of the symbols.

with and without 10 mol % PA, and its dephosphorylation was assessed by electrophoretic mobility in Phos-tag SDS-PAGE. Compared with Nem1-Spo7 phosphatase activity in the presence of PA, the enzyme activity was lower in the absence of PA as reflected by a less increase in Pah1 mobility (**Fig. 6**A). The stimulatory effect of PA on Nem1-Spo7 phosphatase was further examined using the radioactive assay with Pah1 phosphorylated by Pho85-Pho80 with [γ-^{32}P]ATP. The phosphatase complex was reconstituted in a series of phospholipid vesicles containing varying amounts of PA. Compared with Nem1-Spo7 activity in the absence of PA, the enzyme activity was stimulated by the phospholipid in a cooperative dose-dependent manner (Fig. 6B). Analysis of the data yielded a Hill number of ~1.5. The Nem1-Spo7 phosphatase activity in the presence of 10 mol % PA was 3.6-fold greater than the enzyme activity in the absence of PA (Fig. 6B, C). In contrast to PA, thioPA (1, 2-diacyl-sn-glycero-3-phosphorothioate) containing a sulfur atom in place of an oxygen in the phosphate headgroup did not show a significant stimulatory effect on Nem1-Spo7 phosphatase activity (Fig. 6C). Similarly, the PAP product DAG substituted for PA in the proteoliposome did not stimulate the Nem1-Spo7 phosphatase activity (Fig. 6C, *control*). The stimulatory effect of PA was not affected by the composition of its fatty acyl groups, which include two saturated (16:0 to 16:0), two mono-unsaturated (18:1 to 18:1), or one saturated and one

unsaturated (18:0-18:1) fatty acyl chains (Fig. 6D). Overall, these results indicate that the stimulatory effect of PA on Nem1-Spo7 phosphatase is governed by the phosphate headgroup but not by the fatty acyl groups of the phospholipid.

The Nem1-Spo7/Pah1 phosphatase cascade is reconstituted with proteoliposomes

After confirming that Nem1-Spo7 proteoliposomes are active on phosphorylated Pah1, we sought to establish the phosphatase cascade in the reconstituted assay system. For this experiment, the Nem1-Spo7 complex was reconstituted in phospholipid vesicles containing 10 mol % PA. The proteoliposomes were incubated with Pah1 phosphorylated by Pho85-Pho80 with unlabeled ATP. The reaction mixture was incubated for 45 min at pH 5.0 to allow for the maximum Nem1-Spo7 activity on phosphorylated Pah1 and to compensate for the reduced PAP activity of dephosphorylated Pah1 at pH 5.0 when compared with its optimum at pH 7.0–7.5 (35, 116). An intermediate pH between the optimums for Nem1-Spo7 and Pah1 was not used for the assay because the former activity drops precipitously at pH above 5.0 (70). The amounts of PA and DAG in the proteasomes were determined at the 0- and 45-min time intervals to assess the course of the PAP reaction. After the 45-min incubation, the amount of DAG produced was 0.7 nmol (**Fig. 7**), corresponding to 17% of PA dephosphorylation from its total vesicle concentration of 4.2 nmol. Considering the accessible amount of PA in the vesicles, its conversion to DAG would be 34% based on the equal distribution of the phospholipid between the inner and outer leaflets. As expected, DAG was not produced from the reaction when PA was omitted from the Nem1-Spo7 proteoliposomes. Moreover, the catalytic site mutant Pah1-D398E (83) (Fig. 7, *inset*) did not produce DAG in the reconstituted assay system. Taken together, these results demonstrate the control of PAP activity in the reconstituted Nem1-Spo7/Pah1 phosphatase cascade.

DISCUSSION

In the yeast *S. cerevisiae*, Pah1 is a key regulator in lipid synthesis; it controls the bifurcation of PA between DAG and CDP-DAG for the synthesis of the neutral storage lipid TAG and membrane phospholipids, respectively (2, 50–54) (Fig. 1). The physiological function of Pah1 is largely controlled by its cellular location, which is mediated by phosphorylation and dephosphorylation (54). Phosphorylated Pah1 is sequestered in the cytosol apart from its nuclear/ER membrane-associated substrate PA, whereas dephosphorylated Pah1 associates with the membrane to catalyze the PAP reaction to generate DAG (54). Thus, the master regulators of Pah1 function are the protein kinases that phosphorylate Pah1 in the cytosol and the nuclear/ER membrane-associated Nem1-Spo7 protein phosphatase
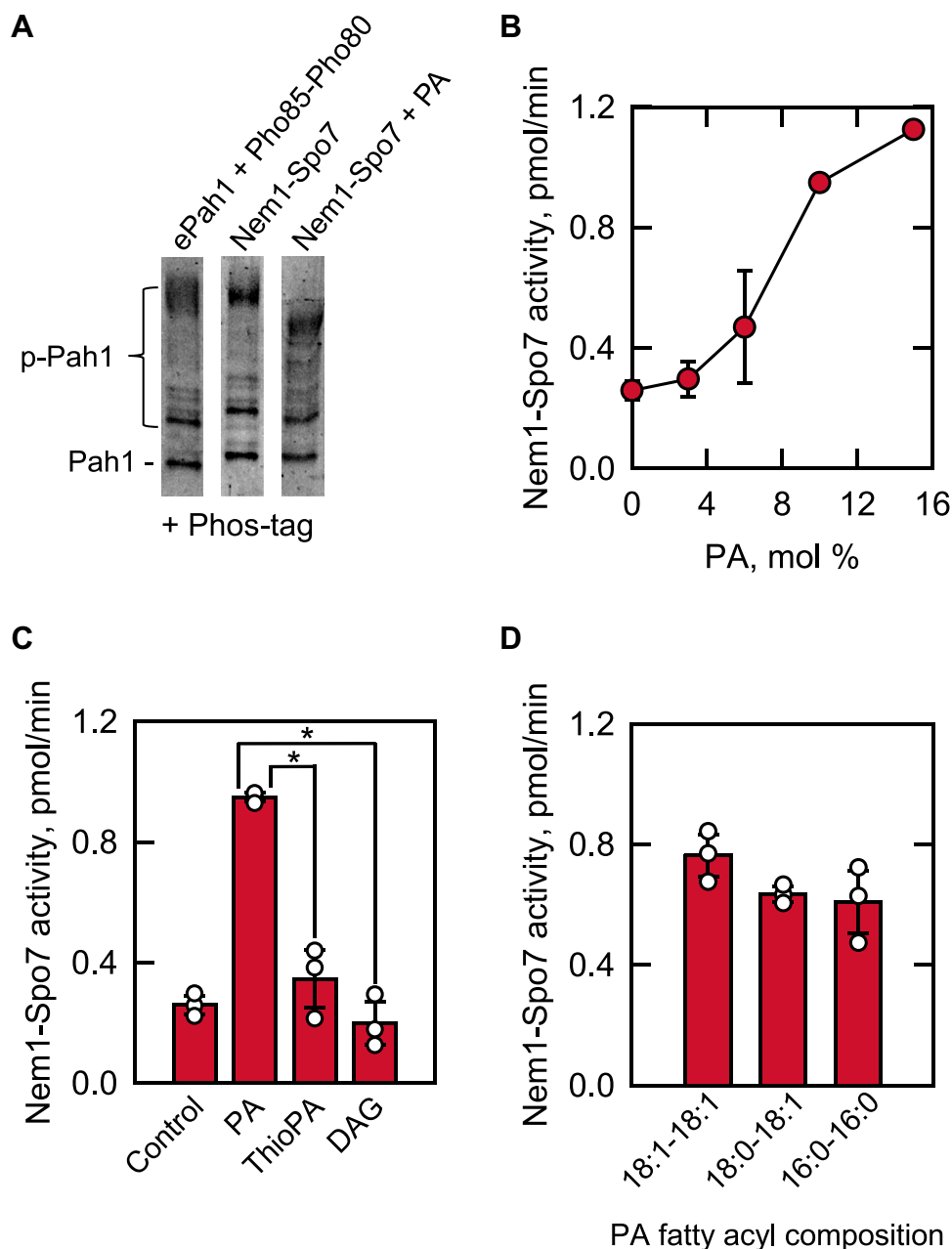
Fig. 6. Nem1-Spo7 protein phosphatase activity is stimulated by PA in proteoliposomes. The Nem1-Spo7 complex was reconstituted into liposomes with or without 10 mol % PA, ThioPA, or DAG, or with 10 mol % PA with different fatty acyl compositions. The *Escherichia coli*-expressed and purified unphosphorylated Pah1 was phosphorylated by Pho85-Pho80 (*ePah1 + Pho85-Pho80*) with unlabeled ATP (A) or [γ-^{32}P]ATP (B–D). The Nem1-Spo7 protein phosphatase activity was measured for 45 min by following the increase in the electrophoretic mobility of Pah1 visualized by staining with Coomassie blue of a 6% SDS-polyacrylamide gel containing 20 μM Phos-tag and 100 μM MnCl$_2$ (A) or the release of ^{32}P$_i$ from [^{32}P]Pah1 (B–D). The data shown in (A) is representative of three experiments, whereas the data in (B–D) are the average of three experiments ± S.D. (*error bars*). The individual data points are shown in (C, D). *, $P < 0.05$ versus PA-containing Nem1-Spo7 proteoliposomes. *Control*, no PA in proteoliposomes. PA, phosphatidate.

complex that recruits and dephosphorylates the enzyme at the membrane (61–65, 70, 71, 73–76). In this work, we developed a model system to examine Pah1 phosphorylation by Pho85-Pho80, the protein kinase that has the greatest effect on Pah1 function (54, 64), and its dephosphorylation by the membrane-associated Nem1-Spo7 protein phosphatase complex.

We successfully reconstituted functional Nem1-Spo7 complex into phospholipid vesicles composed of PC/PE/PI/PS/PA, which constitutes the nuclear/ER membrane bilayer (1, 78, 79). The phospholipid vesicles afford a surface for PAP activity that rivals that of Triton X-100/PA-mixed micelles (77). The average size (60 nm) of the Nem1-Spo7 proteoliposomes prepared by size-exclusion chromatography was similar to that of other proteoliposomes reconstituted with lipid metabolic enzymes prepared by the same method (88–90). Moreover, the lack of latent Nem1-Spo7 activity upon
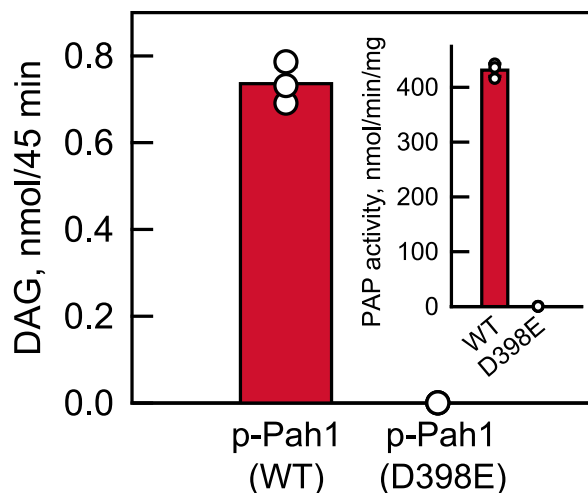
Fig. 7. Reconstitution of the Nem1-Spo7/Pah1 phosphatase cascade in proteoliposomes. The Nem1-Spo7 complex was reconstituted into liposomes with 10 mol % PA. *Escherichia coli*-expressed and purified unphosphorylated WT or D398E forms of Pah1 were phosphorylated by Pho85-Pho80 with unlabeled ATP. The phosphorylated forms of Pah1 were incubated with the Nem1-Spo7 proteoliposomes for 45 min. Following the incubation, the proteoliposomes were collected, the lipids extracted, and the amounts of PA and DAG were analyzed by TLC. *Inset*, unphosphorylated WT and D398E forms of Pah1 were assayed for PAP activity by following the release of P_i from PA using liposomes composed of PC/PE/PI/PS/PA. The surface concentration of PA within the liposomes was 10 mol %. The data shown in the figure is the average of three independent experiments ± S.D. (*error bars*). The error bars are hidden behind the symbols. The individual data points are shown. PA, phosphatidate; PAP, phosphatidate phosphatase.

proteoliposome disruption with detergent indicated that the active site of Nem1 is located at the external side of the vesicle. This model system permitted analysis of the Nem1-Spo7/Pah1 phosphatase cascade starting with the phosphorylation of Pah1 by Pho85-Pho80 and ending with the production of DAG.

Analyzing Nem1-Spo7 proteoliposomes with and without PA revealed that the protein phosphatase activity is stimulated by the PAP substrate. The stimulatory effect of PA was governed by the nature of the phosphate headgroup. For example, thioPA, the phosphorothioate analog of PA, did not stimulate Nem1-Spo7 activity. Parenthetically, thioPA is not a substrate for the PAP reaction (100). Additionally, DAG lacking the phosphate moiety of a phospholipid molecule did not stimulate the protein phosphatase activity. The fatty acyl moiety of PA did not have a significant effect on its stimulatory effect on Nem1-Spo7 activity. Likewise, the PA fatty acyl groups do not affect Pah1 PAP activity (77). The mechanism by which PA stimulates Nem1-Spo7 phosphatase activity is unclear at present. We consider that the stimulatory effect on the enzyme activity might be governed by direct interaction (117) of PA with Nem1 and/or Spo7 and/or by the effect of PA on the membrane bilayer environment (118–121). Additional work is required to address these notions.

The stimulatory effect of PA on Nem1-Spo7 activity was an unexpected finding that has implications for the regulation of the phosphatase cascade affecting the PA/DAG balance and lipid synthesis. We envisage a scenario where the cell senses elevated PA levels that fuel the recruitment and dephosphorylation of Pah1 for its function on the membrane. The activation of Pah1 in turn reduces PA levels through TAG synthesis controlled by its PAP activity. Reduced PA levels would signal the opposite effects such as reduced Nem1-Spo7 activity, Pah1 hyperphosphorylation, and reduced PAP activity. This situation, however, may be an over-simplification of the complex regulation that occurs in vivo with multiple lipid biosynthetic enzymes (e.g., glycerol-3-phosphate and lysoPA acyltransferases, DAG kinase, and phospholipase D) that affect PA levels (2–4, 122).

In addition to being a phospholipid intermediate in lipid biosynthetic pathways (Fig. 1), PA itself functions as a signaling molecule in various cellular functions. In mammalian cells, PA activates cell growth and proliferation, vesicular trafficking, secretion, endocytosis, and even hair growth (123–130). In plants, PA is implicated in seed germination and stress responses to low temperature, salinity, and drought (125, 126). In bacteria, PA plays a role in signaling and biofilm formation (131). In yeast, PA is required for suppression of the growth and membrane trafficking defects in the Sec14 PI/PC binding protein mutant (132–134) and in Spo20-mediated fusion of vesicles with the prespore membrane during sporogenesis (135, 136). Most germane to the control of lipid synthesis in yeast is the role of PA in the expression of lipid synthesis genes via the Henry (Opi1/Ino2-Ino4) regulatory circuit (2–4, 137). PA, along with Scs2, has the ability to sequester the Opi1 repressor at the nuclear/ER membrane, permitting the Ino2-Ino4 complex-mediated transcriptional activation of UAS_{INO}-containing phospholipid synthesis genes (2–4, 137). Reduced PA levels permit Opi1 to dissociate from the nuclear/ER membrane and translocate into the nucleus where it interacts with Ino2 to attenuate transcription of UAS_{INO}-containing genes (2–4, 137).

The Pah1-mediated control of PA plays an important role in the transcriptional regulation of lipid synthesis genes (e.g., *INO1*, *INO2*, *CHO1*, and *OPI3*) via the Henry regulatory circuit (61, 62, 138, 139). We posit that the PA-mediated regulation of the Nem1-Spo7 phosphatase complex must be involved in this regulation. Interestingly, the fatty acyl species of PA do not stimulate the Nem1-Spo7 and PAP activities but affect the interaction of Opi1 with the phospholipid; the PA species 34:1, the most abundant PA species in *S. cerevisiae* (33), mediates expression of the UAS_{INO}-containing *INO1* gene (139). In addition, the Opi1 repressor function is also affected by the fatty acyl chain length of PA; Opi1 binding to PA is favored with its C16- over C18-chain length (140).

The reconstitution of the Nem1-Spo7/Pah1 axis is a significant advance in modeling a regulatory cascade in

lipid synthesis. This proteoliposome system will permit well-defined studies to examine the structure-function relationships of Nem1, Spo7, and Pah1 as well as the phosphorylation-mediated interactions of Pah1 with the Nem1-Spo7 complex at the membrane surface. In fact, in a recent study, the system provided important information on Nem1-Spo7 activity on Pah1 phosphorylated by Pho85-Pho80 and glycogen synthase kinase homolog Rim11, which showed a preference for dephosphorylating target sites of the Pho85-Pho80 protein kinase (69).

Data Availability

All data are contained within the article or supporting information.⬛

Author ORCIDs

Joanna M. Kwiatek ⓘ https://orcid.org/0000-0001-8934-0922
Bryan Gutierrez ⓘ https://orcid.org/0000-0003-2351-5608
Enver Cagri Izgu ⓘ https://orcid.org/0000-0001-6673-3635
Gil-Soo Han ⓘ https://orcid.org/0000-0002-8170-854X
George M. Carman ⓘ https://orcid.org/0000-0003-4951-8233

Conflict of Interest

The authors declare that they have no conflicts of interest with the contents of this article.

REFERENCES

1. Rattray, J. B., Schibeci, A., and Kidby, D. K. (1975) Lipids of yeast. *Bacteriol. Rev.* **39**, 197–231
2. Kwiatek, J. M., Han, G. S., and Carman, G. M. (2020) Phosphatidate-mediated regulation of lipid synthesis at the nuclear/endoplasmic reticulum membrane. *Biochim. Biophys. Acta Mol. Cell Biol. Lipids.* **1865**, 158434
3. Carman, G. M., and Han, G-S. (2011) Regulation of phospholipid synthesis in the yeast *Saccharomyces cerevisiae. Ann. Rev. Biochem.* **80**, 859–883
4. Henry, S. A., Kohlwein, S., and Carman, G. M. (2012) Metabolism and regulation of glycerolipids in the yeast *Saccharomyces cerevisiae. Genetics.* **190**, 317–349
5. Carman, G. M. (2021) Lipid metabolism has been good to me. *J. Biol. Chem.* **297**, 100786
6. Athenstaedt, K., and Daum, G. (1997) Biosynthesis of phosphatidic acid in lipid particles and endoplasmic reticulum of *Saccharomyces cerevisiae. J. Bacteriol.* **179**, 7611–7616
7. Athenstaedt, K., Weys, S., Paltauf, F., and Daum, G. (1999) Redundant systems of phosphatidic acid biosynthesis via acylation of glycerol-3-phosphate or dihydroxyacetone phosphate in the yeast *Saccharomyces cerevisiae. J. Bacteriol.* **181**, 1458–1463
8. Zheng, Z., and Zou, J. (2001) The initial step of the glycerolipid pathway: identification of glycerol 3-phosphate/dihydroxyacetone phosphate dual substrate acyltransferases in *Saccharomyces cerevisiae. J. Biol. Chem.* **276**, 41710–41716
9. Riekhof, W. R., Wu, J., Jones, J. L., and Voelker, D. R. (2007) Identification and characterization of the major lysophosphatidylethanolamine acyltransferase in *Saccharomyces cerevisiae. J. Biol. Chem.* **282**, 28344–28352
10. Jain, S., Stanford, N., Bhagwat, N., Seiler, B., Costanzo, M., Boone, C., *et al.* (2007) Identification of a novel lysophospholipid acyltransferase in *Saccharomyces cerevisiae. J. Biol. Chem.* **282**, 30562–30569
11. Benghezal, M., Roubaty, C., Veepuri, V., Knudsen, J., and Conzelmann, A. (2007) *SLC1* and *SLC4* encode partially redundant acyl-coenzyme A 1-acylglycerol-3-phosphate O-Acyltransferases of budding yeast. *J. Biol. Chem.* **282**, 30845–30855
12. Chen, Q., Kazachkov, M., Zheng, Z., and Zou, J. (2007) The yeast acylglycerol acyltransferase LCA1 is a key component of Lands cycle for phosphatidylcholine turnover. *FEBS Lett.* **581**, 5511–5516
13. Carter, J. R., and Kennedy, E. P. (1966) Enzymatic synthesis of cytidine diphosphate diglyceride. *J. Lipid Res.* **7**, 678–683
14. Shen, H., Heacock, P. N., Clancey, C. J., and Dowhan, W. (1996) The *CDS1* gene encoding CDP-diacylglycerol synthase in *Saccharomyces cerevisiae* is essential for cell growth. *J. Biol. Chem.* **271**, 789–795
15. Paulus, H., and Kennedy, E. P. (1960) The enzymatic synthesis of inositol monophosphatide. *J. Biol. Chem.* **235**, 1303–1311
16. Nikawa, J., and Yamashita, S. (1984) Molecular cloning of the gene encoding CDP-diacylglycerol- inositol 3-phosphatidyl transferase in *Saccharomyces cerevisiae. Eur. J. Biochem.* **143**, 251–256
17. Nikawa, J., Kodaki, T., and Yamashita, S. (1987) Primary structure and disruption of the phosphatidylinositol synthase gene of *Saccharomyces cerevisiae. J. Biol. Chem.* **262**, 4876–4881
18. Kanfer, J. N., and Kennedy, E. P. (1964) Metabolism and function of bacterial lipids. II. Biosynthesis of phospholipids in *Escherichia coli. J. Biol. Chem.* **239**, 1720–1726
19. Letts, V. A., Klig, L. S., Bae-Lee, M., Carman, G. M., and Henry, S. A. (1983) Isolation of the yeast structural gene for the membrane-associated enzyme phosphatidylserine synthase. *Proc. Natl. Acad. Sci. U. S. A.* **80**, 7279–7283

20. Nikawa, J., Tsukagoshi, Y., Kodaki, T., and Yamashita, S. (1987) Nucleotide sequence and characterization of the yeast *PSS* gene encoding phosphatidylserine synthase. *Eur. J. Biochem.* **167**, 7–12

21. Kiyono, K., Miura, K., Kushima, Y., Hikiji, T., Fukushima, M., Shibuya, I., *et al.* (1987) Primary structure and product characterization of the *Saccharomyces cerevisiae CHO1* gene that encodes phosphatidylserine synthase. *J. Biochem.* **102**, 1089–1100

22. Kannan, M., Lahiri, S., Liu, L. K., Choudhary, V., and Prinz, W. A. (2017) Phosphatidylserine synthesis at membrane contact sites promotes its transport out of the ER. *J. Lipid Res.* **58**, 553–562

23. Miyata, N., Watanabe, Y., Tamura, Y., Endo, T., and Kuge, O. (2016) Phosphatidylserine transport by Ups2-Mdm35 in respiration-active mitochondria. *J. Cell Biol.* **214**, 77–88

24. Clancey, C. J., Chang, S-C., and Dowhan, W. (1993) Cloning of a gene (*PSD1*) encoding phosphatidylserine decarboxylase from *Saccharomyces cerevisiae* by complementation of an *Escherichia coli* mutant. *J. Biol. Chem.* **268**, 24580–24590

25. Trotter, P. J., Pedretti, J., and Voelker, D. R. (1993) Phosphatidylserine decarboxylase from *Saccharomyces cerevisiae*. Isolation of mutants, cloning of the gene, and creation of a null allele. *J. Biol. Chem.* **268**, 21416–21424

26. Bremer, J., and Greenberg, D. M. (1961) Methyl transferring enzyme system of microsomes in the biosynthesis of lecithin (phosphatidylcholine). *Biochim. Biophys. Acta.* **46**, 205–216

27. Kodaki, T., and Yamashita, S. (1987) Yeast phosphatidylethanolamine methylation pathway: cloning and characterization of two distinct methyltransferase genes. *J. Biol. Chem.* **262**, 15428–15435

28. Summers, E. F., Letts, V. A., McGraw, P., and Henry, S. A. (1988) *Saccharomyces cerevisiae cho2* mutants are deficient in phospholipid methylation and cross-pathway regulation of inositol synthesis. *Genetics.* **120**, 909–922

29. McGraw, P., and Henry, S. A. (1989) Mutations in the *Saccharomyces cerevisiae OPI3* gene: effects on phospholipid methylation, growth, and cross pathway regulation of phospholipid synthesis. *Genetics.* **122**, 317–330

30. Taylor, F. R., and Parks, L. W. (1979) Triacylglycerol metabolism in *Saccharomyces cerevisiae* relation to phospholipid synthesis. *Biochim. Biophys. Acta.* **575**, 204–214

31. Pascual, F., Soto-Cardalda, A., and Carman, G. M. (2013) *PAH1*-encoded phosphatidate phosphatase plays a role in the growth phase- and inositol-mediated regulation of lipid synthesis in *Saccharomyces cerevisiae*. *J. Biol. Chem.* **288**, 35781–35792

32. Adeyo, O., Horn, P. J., Lee, S., Binns, D. D., Chandrahas, A., Chapman, K. D., *et al.* (2011) The yeast lipin orthologue Pah1p is important for biogenesis of lipid droplets. *J. Cell Biol.* **192**, 1043–1055

33. Fakas, S., Qiu, Y., Dixon, J. L., Han, G-S., Ruggles, K. V., Garbarino, J., *et al.* (2011) Phosphatidate phosphatase activity plays a key role in protection against fatty acid-induced toxicity in yeast. *J. Biol. Chem.* **286**, 29074–29085

34. Smith, S. W., Weiss, S. B., and Kennedy, E. P. (1957) The enzymatic dephosphorylation of phosphatidic acids. *J. Biol. Chem.* **228**, 915–922

35. Han, G-S., Wu, W-I., and Carman, G. M. (2006) The *Saccharomyces cerevisiae* lipin homolog is a Mg^{2+}-dependent phosphatidate phosphatase enzyme. *J. Biol. Chem.* **281**, 9210–9218

36. Atkinson, K., Fogel, S., and Henry, S. A. (1980) Yeast mutant defective in phosphatidylserine synthesis. *J. Biol. Chem.* **255**, 6653–6661

37. Atkinson, K. D., Jensen, B., Kolat, A. I., Storm, E. M., Henry, S. A., and Fogel, S. (1980) Yeast mutants auxotropic for choline or ethanolamine. *J. Bacteriol.* **141**, 558–564

38. Trotter, P. J., Pedretti, J., Yates, R., and Voelker, D. R. (1995) Phosphatidylserine decarboxylase 2 of *Saccharomyces cerevisiae*. Cloning and mapping of the gene, heterologous expression, and creation of the null allele. *J. Biol. Chem.* **270**, 6071–6080

39. Trotter, P. J., and Voelker, D. R. (1995) Identification of a non-mitochondrial phosphatidylserine decarboxylase activity (*PSD2*) in the yeast *Saccharomyces cerevisiae*. *J. Biol. Chem.* **270**, 6062–6070

40. Kodaki, T., and Yamashita, S. (1989) Characterization of the methyltransferases in the yeast phosphatidylethanolamine methylation pathway by selective gene disruption. *Eur. J. Biochem.* **185**, 243–251

41. Kim, K., Kim, K-H., Storey, M. K., Voelker, D. R., and Carman, G. M. (1999) Isolation and characterization of the *Saccharomyces cerevisiae EKI1* gene encoding ethanolamine kinase. *J. Biol. Chem.* **274**, 14857–14866

42. Min-Seok, R., Kawamata, Y., Nakamura, H., Ohta, A., and Takagi, M. (1996) Isolation and characterization of *ECT1* gene encoding CTP:phosphoethanolamine cytidylyltransferase of *Saccharomyces cerevisiae*. *J. Biochem.* **120**, 1040–1047

43. Hjelmstad, R. H., and Bell, R. M. (1988) The *sn*-1,2-diacylglycerol ethanolaminephosphotransferase of *Saccharomyces cerevisiae*. Isolation of mutants and cloning of the *EPT1* gene. *J. Biol. Chem.* **263**, 19748–19757

44. Hjelmstad, R. H., and Bell, R. M. (1991) *sn*-1,2-diacylglycerol choline- and ethanolaminephosphotransferases in *Saccharomyces cerevisiae*. Nucleotide sequence of the *EPT1* gene and comparison of the *CPT1* and *EPT1* gene products. *J. Biol. Chem.* **266**, 5094–5103

45. Hosaka, K., Kodaki, T., and Yamashita, S. (1989) Cloning and characterization of the yeast *CKI* gene encoding choline kinase and its expression in *Escherichia coli*. *J. Biol. Chem.* **264**, 2053–2059

46. Tsukagoshi, Y., Nikawa, J., and Yamashita, S. (1987) Molecular cloning and characterization of the gene encoding cholinephosphate cytidylyltransferase in *Saccharomyces cerevisiae*. *Eur. J. Biochem.* **169**, 477–486

47. Hjelmstad, R. H., and Bell, R. M. (1987) Mutants of *Saccharomyces cerevisiae* defective in sn-1,2- diacylglycerol cholinephosphotransferase: isolation, characterization, and cloning of the *CPT1* gene. *J. Biol. Chem.* **262**, 3909–3917

48. Hjelmstad, R. H., and Bell, R. M. (1990) The *sn*-1,2-diacylglycerol cholinephosphotransferase of *Saccharomyces cerevisiae*. Nucleotide sequence, transcriptional mapping, and gene product analysis of the *CPT1* gene. *J. Biol. Chem.* **265**, 1755–1764

49. Romanauska, A., and Kohler, A. (2018) The inner nuclear membrane Is a metabolically active territory that generates nuclear lipid droplets. *Cell.* **174**, 700–715

50. Carman, G. M., and Han, G-S. (2006) Roles of phosphatidate phosphatase enzymes in lipid metabolism. *Trends Biochem. Sci.* **31**, 694–699

51. Carman, G. M., and Han, G-S. (2009) Phosphatidic acid phosphatase, a key enzyme in the regulation of lipid synthesis. *J. Biol. Chem.* **284**, 2593–2597

52. Pascual, F., and Carman, G. M. (2013) Phosphatidate phosphatase, a key regulator of lipid homeostasis. *Biochim. Biophys. Acta.* **1831**, 514–522

53. Carman, G. M., and Han, G. S. (2019) Fat-regulating phosphatidic acid phosphatase: a review of its roles and regulation in lipid homeostasis. *J. Lipid Res.* **60**, 2–6

54. Khondker, S., Han, G-S., and Carman, G. M. (2022) Phosphorylation-mediated regulation of the Nem1-Spo7/Pah1 phosphatase cascade in yeast lipid synthesis. *Adv. Biol. Regul.* **84**, 100889

55. Park, Y., Han, G. S., Mileykovskaya, E., Garrett, T. A., and Carman, G. M. (2015) Altered lipid synthesis by lack of yeast Pah1 phosphatidate phosphatase reduces chronological life span. *J. Biol. Chem.* **290**, 25382–25394

56. Carman, G. M. (2018) Discoveries of the phosphatidate phosphatase genes in yeast published in the Journal of Biological Chemistry. *J. Biol. Chem.* **294**, 1681–1689

57. Soto-Cardalda, A., Fakas, S., Pascual, F., Choi, H. S., and Carman, G. M. (2011) Phosphatidate phosphatase plays role in zinc-mediated regulation of phospholipid synthesis in yeast. *J. Biol. Chem.* **287**, 968–977

58. Wu, W-I., and Carman, G. M. (1996) Regulation of phosphatidate phosphatase activity from the yeast *Saccharomyces cerevisiae* by phospholipids. *Biochemistry.* **35**, 3790–3796

59. Wu, W-I., Lin, Y-P., Wang, E., Merrill, A. H., Jr., and Carman, G. M. (1993) Regulation of phosphatidate phosphatase activity from the yeast *Saccharomyces cerevisiae* by sphingoid bases. *J. Biol. Chem.* **268**, 13830–13837

60. Wu, W-I., and Carman, G. M. (1994) Regulation of phosphatidate phosphatase activity from the yeast *Saccharomyces cerevisiae* by nucleotides. *J. Biol. Chem.* **269**, 29495–29501

61. Santos-Rosa, H., Leung, J., Grimsey, N., Peak-Chew, S., and Siniossoglou, S. (2005) The yeast lipin Smp2 couples phospholipid biosynthesis to nuclear membrane growth. *EMBO J.* **24**, 1931–1941

62. O'Hara, L., Han, G-S., Peak-Chew, S., Grimsey, N., Carman, G. M., and Siniossoglou, S. (2006) Control of phospholipid synthesis by phosphorylation of the yeast lipin Pah1p/Smp2p Mg^{2+}-dependent phosphatidate phosphatase. *J. Biol. Chem.* **281**, 34537–34548

63. Choi, H-S., Su, W-M., Morgan, J. M., Han, G-S., Xu, Z., Karanasios, E., *et al.* (2011) Phosphorylation of phosphatidate phosphatase regulates its membrane association and physiological functions in *Saccharomyces cerevisiae:* identification of Ser^{602}, Thr^{723}, and Ser^{744} as the sites phosphorylated by *CDC28 (CDK1)*-encoded cyclin-dependent kinase. *J. Biol. Chem.* **286**, 1486–1498

64. Choi, H-S., Su, W-M., Han, G-S., Plote, D., Xu, Z., and Carman, G. M. (2012) Pho85p-Pho80p phosphorylation of yeast Pah1p phosphatidate phosphatase regulates its activity, location, abundance, and function in lipid metabolism. *J. Biol. Chem.* **287**, 11290–11301

65. Su, W-M., Han, G-S., Casciano, J., and Carman, G. M. (2012) Protein kinase A-mediated phosphorylation of Pah1p phosphatidate phosphatase functions in conjunction with the Pho85p-Pho80p and Cdc28p-cyclin B kinases to regulate lipid synthesis in yeast. *J. Biol. Chem.* **287**, 33364–33376

66. Su, W-M., Han, G-S., and Carman, G. M. (2014) Cross-talk phosphorylations by protein kinase C and Pho85p-Pho80p protein kinase regulate Pah1p phosphatidate phosphatase abundance in *Saccharomyces cerevisiae*. *J. Biol. Chem.* **289**, 18818–18830

67. Hsieh, L-S., Su, W-M., Han, G-S., and Carman, G. M. (2016) Phosphorylation of yeast Pah1 phosphatidate phosphatase by casein kinase II regulates its function in lipid metabolism. *J. Biol. Chem.* **291**, 9974–9990

68. Hassaninasab, A., Hsieh, L. S., Su, W. M., Han, G. S., and Carman, G. M. (2019) Yck1 casein kinase I regulates the activity and phosphorylation of Pah1 phosphatidate phosphatase from *Saccharomyces cerevisiae*. *J. Biol. Chem.* **294**, 18256–18268

69. Khondker, S., Kwiatek, J. M., Han, G. S., and Carman, G. M. (2022) Glycogen synthase kinase homolog Rim11 regulates lipid synthesis through the phosphorylation of Pah1 phosphatidate phosphatase in yeast. *J. Biol. Chem.* **298**, 102221

70. Su, W-M., Han, G-S., and Carman, G. M. (2014) Yeast Nem1-Spo7 protein phosphatase activity on Pah1 phosphatidate phosphatase is specific for the Pho85-Pho80 protein kinase phosphorylation sites. *J. Biol. Chem.* **289**, 34699–34708

71. Siniossoglou, S., Santos-Rosa, H., Rappsilber, J., Mann, M., and Hurt, E. (1998) A novel complex of membrane proteins required for formation of a spherical nucleus. *EMBO J.* **17**, 6449–6464

72. Hsieh, L-S., Su, W-M., Han, G-S., and Carman, G. M. (2015) Phosphorylation regulates the ubiquitin-independent degradation of yeast Pah1 phosphatidate phosphatase by the 20S proteasome. *J. Biol. Chem.* **290**, 11467–11478

73. Karanasios, E., Han, G-S., Xu, Z., Carman, G. M., and Siniossoglou, S. (2010) A phosphorylation-regulated amphipathic helix controls the membrane translocation and function of the yeast phosphatidate phosphatase. *Proc. Natl. Acad. Sci. U. S. A.* **107**, 17539–17544

74. Karanasios, E., Barbosa, A. D., Sembongi, H., Mari, M., Han, G-S., Reggiori, F., *et al.* (2013) Regulation of lipid droplet and membrane biogenesis by the acidic tail of the phosphatidate phosphatase Pah1p. *Mol. Biol. Cell.* **24**, 2124–2133

75. Xu, Z., Su, W-M., and Carman, G. M. (2012) Fluorescence spectroscopy measures yeast *PAH1*-encoded phosphatidate phosphatase interaction with liposome membranes. *J. Lipid Res.* **53**, 522–528

76. Barbosa, A. D., Sembongi, H., Su, W-M., Abreu, S., Reggiori, F., Carman, G. M., *et al.* (2015) Lipid partitioning at the nuclear envelope controls membrane biogenesis. *Mol. Biol. Cell.* **26**, 3641–3657

77. Kwiatek, J. M., and Carman, G. M. (2020) Yeast phosphatidic acid phosphatase Pah1 hops and scoots along the membrane phospholipid bilayer. *J. Lipid Res.* **61**, 1232–1243

78. Henry, S. A. (1982) Membrane lipids of yeast: biochemical and genetic studies. In *The molecular biology of the yeast Saccharomyces. Metabolism and gene expression*. J. N. Strathern, E. W. Jones, and J. R. Broach, editors. Cold Spring Harbor Laboratory, Cold Spring Harbor, 101–158

79. Zinser, E., Sperka-Gottlieb, C. D. M., Fasch, E-V., Kohlwein, S. D., Paltauf, F., and Daum, G. (1991) Phospholipid synthesis and lipid composition of subcellular membranes in the unicellular eukaryote *Saccharomyces cerevisiae*. *J. Bacteriol.* **173**, 2026–2034

80. Su, W-M., Han, G. S., Dey, P., and Carman, G. M. (2018) Protein kinase A phosphorylates the Nem1-Spo7 protein phosphatase complex that regulates the phosphorylation state of the phosphatidate phosphatase Pah1 in yeast. *J. Biol. Chem.* **293**, 15801–15814

81. Wimmer, C., Doye, V., Grandi, P., Nehrbass, U., and Hurt, E. C. (1992) A new subclass of nucleoporins that functionally interact with nuclear pore protein NSP1. *EMBO J.* **11**, 5051–5061

82. Han, G-S., O'Hara, L., Carman, G. M., and Siniossoglou, S. (2008) An unconventional diacylglycerol kinase that regulates phospholipid synthesis and nuclear membrane growth. *J. Biol. Chem.* **283**, 20433–20442

83. Han, G-S., Siniossoglou, S., and Carman, G. M. (2007) The cellular functions of the yeast lipin homolog Pah1p are dependent on its phosphatidate phosphatase activity. *J. Biol. Chem.* **282**, 37026–37035

84. Jeffery, D. A., Springer, M., King, D. S., and O'Shea, E. K. (2001) Multi-site phosphorylation of Pho4 by the cyclin-CDK Pho80-Pho85 is semi-processive with site preference. *J. Mol. Biol.* **306**, 997–1010

85. Siniossoglou, S., Hurt, E. C., and Pelham, H. R. (2000) Psr1p/Psr2p, two plasma membrane phosphatases with an essential DXDX(T/V) motif required for sodium stress response in yeast. *J. Biol. Chem.* **275**, 19352–19360

86. Park, Y., Stukey, G. J., Jog, R., Kwiatek, J. M., Han, G. S., and Carman, G. M. (2022) Mutant phosphatidate phosphatase Pah1-W637A exhibits altered phosphorylation, membrane association, and enzyme function in yeast. *J. Biol. Chem.* **101578**

87. Mimms, L. T., Zamphighi, G., Nozaki, Y., Tanford, C., and Reynolds, J. A. (1981) Phospholipid vesicle formation and transmembrane protein incorporation using octylglucoside. *Biochemistry.* **20**, 833–840

88. Green, P. R., and Bell, R. M. (1984) Asymmetric reconstitution of homogeneous *Escherichia coli* sn- glycerol-3-phosphate acyltransferase into phospholipid vesicles. *J. Biol. Chem.* **259**, 14688–14694

89. Fischl, A. S., Homann, M. J., Poole, M. A., and Carman, G. M. (1986) Phosphatidylinositol synthase from *Saccharomyces cerevisiae*. Reconstitution, characterization, and regulation of activity. *J. Biol. Chem.* **261**, 3178–3183

90. Hromy, J. M., and Carman, G. M. (1986) Reconstitution of *Saccharomyces cerevisiae* phosphatidylserine synthase into phospholipid vesicles. Modulation of activity by phospholipids. *J. Biol. Chem.* **261**, 15572–15576

91. Bligh, E. G., and Dyer, W. J. (1959) A rapid method of total lipid extraction and purification. *Can. J. Biochem. Physiol.* **37**, 911–917

92. Vaden, D. L., Gohil, V. M., Gu, Z., and Greenberg, M. L. (2005) Separation of yeast phospholipids using one-dimensional thin-layer chromatography. *Anal. Biochem.* **338**, 162–164

93. Henderson, R. J., and Tocher, D. R. (1992) Thin-layer chromatography. In *Lipid Analysis*. R. J. Hamilton and S. Hamilton, editors. IRL Press, New York, 65–111

94. Mirheydari, M., Dey, P., Stukey, G. J., Park, Y., Han, G. S., and Carman, G. M. (2020) The Spo7 sequence LLI is required for Nem1-Spo7/Pah1 phosphatase cascade function in yeast lipid metabolism. *J. Biol. Chem.* **295**, 11473–11485

95. Laemmli, U. K. (1970) Cleavage of structural proteins during the assembly of the head of bacteriophage T4. *Nature.* **227**, 680–685

96. Havriluk, T., Lozy, F., Siniossoglou, S., and Carman, G. M. (2007) Colorimetric determination of pure Mg^{2+}-dependent phosphatidate phosphatase activity. *Anal. Biochem.* **373**, 392–394

97. Han, G-S., and Carman, G. M. (2010) Characterization of the human *LPIN1*-encoded phosphatidate phosphatase isoforms. *J. Biol. Chem.* **285**, 14628–14638

98. Burnette, W. (1981) Western blotting: electrophoretic transfer of proteins from sodium dodecyl sulfate-polyacrylamide gels to unmodified nitrocellulose and radiographic detection with antibody and radioiodinated protein A. *Anal. Biochem.* **112**, 195–203

99. Haid, A., and Suissa, M. (1983) Immunochemical identification of membrane proteins after sodium dodecyl sulfate-polyacrylamide gel electrophoresis. *Met. Enzymol.* **96**, 192–205

100. Bonnel, S. I., Lin, Y-P., Kelley, M. J., Carman, G. M., and Eichberg, J. (1989) Interactions of thiophosphatidic acid with

enzymes which metabolize phosphatidic acid. Inhibition of phosphatidic acid phosphatase and utilization by CDP-diacylglycerol synthase. *Biochim. Biophys. Acta.* **1005**, 289–295

101. Dubots, E., Cottier, S., Peli-Gulli, M. P., Jaquenoud, M., Bontron, S., Schneiter, R., *et al.* (2014) TORC1 regulates Pah1 phosphatidate phosphatase activity via the Nem1/Spo7 protein phosphatase complex. *PLoS. One.* **9**, e104194

102. Gruhler, A., Olsen, J. V., Mohammed, S., Mortensen, P., Faergeman, N. J., Mann, M., *et al.* (2005) Quantitative phosphoproteomics applied to the yeast pheromone signaling pathway. *Mol. Cell Proteomics.* **4**, 310–327

103. Li, X., Gerber, S. A., Rudner, A. D., Beausoleil, S. A., Haas, W., Villen, J., *et al.* (2007) Large-scale phosphorylation analysis of alpha-factor-arrested *Saccharomyces cerevisiae.* *J. Proteome. Res.* **6**, 1190–1197

104. Chi, A., Huttenhower, C., Geer, L. Y., Coon, J. J., Syka, J. E., Bai, D. L., *et al.* (2007) Analysis of phosphorylation sites on proteins from *Saccharomyces cerevisiae* by electron transfer dissociation (ETD) mass spectrometry. *Proc. Natl. Acad. Sci. U. S. A.* **104**, 2193–2198

105. Smolka, M. B., Albuquerque, C. P., Chen, S. H., and Zhou, H. (2007) Proteome-wide identification of in vivo targets of DNA damage checkpoint kinases. *Proc. Natl. Acad. Sci. U. S. A.* **104**, 10364–10369

106. Albuquerque, C. P., Smolka, M. B., Payne, S. H., Bafna, V., Eng, J., and Zhou, H. (2008) A multidimensional chromatography technology for in-depth phosphoproteome analysis. *Mol. Cell Proteomics.* **7**, 1389–1396

107. Soufi, B., Kelstrup, C. D., Stoehr, G., Frohlich, F., Walther, T. C., and Olsen, J. V. (2009) Global analysis of the yeast osmotic stress response by quantitative proteomics. *Mol. Biosyst.* **5**, 1337–1346

108. Gnad, F., de Godoy, L. M., Cox, J., Neuhauser, N., Ren, S., Olsen, J. V., *et al.* (2009) High-accuracy identification and bioinformatic analysis of in vivo protein phosphorylation sites in yeast. *Proteomics.* **9**, 4642–4652

109. Helbig, A. O., Rosati, S., Pijnappel, P. W., van, B. B., Timmers, M. H., Mohammed, S., *et al.* (2010) Perturbation of the yeast N-acetyltransferase NatB induces elevation of protein phosphorylation levels. *BMC. Genomics.* **11**, 685

110. Soulard, A., Cremonesi, A., Moes, S., Schutz, F., Jeno, P., and Hall, M. N. (2010) The rapamycin-sensitive phosphoproteome reveals that TOR controls protein kinase A toward some but not all substrates. *Mol. Biol. Cell.* **21**, 3475–3486

111. Bodenmiller, B., Wanka, S., Kraft, C., Urban, J., Campbell, D., Pedrioli, P. G., *et al.* (2010) Phosphoproteomic analysis reveals interconnected system-wide responses to perturbations of kinases and phosphatases in yeast. *Sci. Signal.* **3**, rs4

112. Swaney, D. L., Beltrao, P., Starita, L., Guo, A., Rush, J., Fields, S., *et al.* (2013) Global analysis of phosphorylation and ubiquitylation cross-talk in protein degradation. *Nat. Met.* **10**, 676–682

113. Lanz, M. C., Yugandhar, K., Gupta, S., Sanford, E. J., Faca, V. M., Vega, S., *et al.* (2021) In-depth and 3-dimensional exploration of the budding yeast phosphoproteome. *EMBO Rep.* **22**, e51121

114. MacGilvray, M. E., Shishkova, E., Place, M., Wagner, E. R., Coon, J. J., and Gasch, A. P. (2020) Phosphoproteome response to dithiothreitol reveals unique versus shared features of *Saccharomyces cerevisiae* stress responses. *J. Proteome. Res.* **19**, 3405–3417

115. Kinoshita, E., Kinoshita-Kikuta, E., Takiyama, K., and Koike, T. (2006) Phosphate-binding tag, a new tool to visualize phosphorylated proteins. *Mol. Cell Proteomics.* **5**, 749–757

116. Lin, Y-P., and Carman, G. M. (1989) Purification and characterization of phosphatidate phosphatase from *Saccharomyces cerevisiae.* *J. Biol. Chem.* **264**, 8641–8645

117. Kooijman, E. E., Tieleman, D. P., Testerink, C., Munnik, T., Rijkers, D. T., Burger, K. N., *et al.* (2007) An electrostatic/hydrogen bond switch as the basis for the specific interaction of phosphatidic acid with proteins. *J. Biol. Chem.* **282**, 11356–11364

118. Demel, R. A., Yin, C. C., Lin, B. Z., and Hauser, H. (1992) Monolayer characteristics and thermal behaviour of phosphatidic acids. *Chem. Phys. Lipids.* **60**, 209–223

119. Putta, P., Rankenberg, J., Korver, R. A., van, W. R., Munnik, T., Testerink, C., *et al.* (2016) Phosphatidic acid binding proteins display differential binding as a function of membrane curvature stress and chemical properties. *Biochim. Biophys. Acta.* **1858**, 2709–2716

120. Garidel, P., Johann, C., and Blume, A. (2011) Non-ideal mixing and fluid-fluid immiscibility in phosphatidic acid-phosphatidylethanolamine mixed bilayers. *Eur. Biophys. J.* **40**, 891–905

121. Garidel, P., Johann, C., and Blume, A. (1997) Nonideal mixing and phase separation in phosphatidylcholine-phosphatidic acid mixtures as a function of acyl chain length and pH. *Biophys. J.* **72**, 2196–2210

122. Carman, G. M., and Henry, S. A. (2007) Phosphatidic acid plays a central role in the transcriptional regulation of glycerophospholipid synthesis in *Saccharomyces cerevisiae.* *J. Biol. Chem.* **282**, 37293–37297

123. Waggoner, D. W., Xu, J., Singh, I., Jasinska, R., Zhang, Q. X., and Brindley, D. N. (1999) Structural organization of mammalian lipid phosphate phosphatases: implications for signal transduction. *Biochim. Biophys. Acta.* **1439**, 299–316

124. Sciorra, V. A., and Morris, A. J. (2002) Roles for lipid phosphate phosphatases in regulation of cellular signaling. *Biochim. Biophys. Acta.* **1582**, 45–51

125. Testerink, C., and Munnik, T. (2005) Phosphatidic acid: a multifunctional stress signaling lipid in plants. *Trends Plant Sci.* **10**, 368–375

126. Wang, X., Devaiah, S. P., Zhang, W., and Welti, R. (2006) Signaling functions of phosphatidic acid. *Prog. Lipid Res.* **45**, 250–278

127. Brindley, D. N. (2004) Lipid phosphate phosphatases and related proteins: signaling functions in development, cell division, and cancer. *J. Cell Biochem.* **92**, 900–912

128. Howe, A. G., and McMaster, C. R. (2006) Regulation of phosphatidylcholine homeostasis by Sec14. *Can. J. Physiol. Pharmacol.* **84**, 29–38

129. Foster, D. A. (2007) Regulation of mTOR by phosphatidic acid? *Cancer Res.* **67**, 1–4

130. Takahashi, T., Kamimura, A., Hamazono-Matsuoka, T., and Honda, S. (2003) Phosphatidic acid has a potential to promote hair growth *in vitro* and *in vivo*, and activates mitogen-activated protein kinase/extracellular signal-regulated kinase kinase in hair epithelial cells. *J. Invest. Dermatol.* **121**, 448–456

131. Groenewold, M. K., Massmig, M., Hebecker, S., Danne, L., Magnowska, Z., Nimtz, M., *et al.* (2018) A phosphatidic acid-binding protein is important for lipid homeostasis and adaptation to anaerobic biofilm conditions in *Pseudomonas aeruginosa.* *Biochem. J.* **475**, 1885–1907

132. Patton-Vogt, J. L., Griac, P., Sreenivas, A., Bruno, V., Dowd, S., Swede, M. J., *et al.* (1997) Role of the yeast phosphatidylinositol/phosphatidylcholine transfer protein (Sec14p) in phosphatidylcholine turnover and *INO1* regulation. *J. Biol. Chem.* **272**, 20873–20883

133. Sreenivas, A., Patton-Vogt, J. L., Bruno, V., Griac, P., and Henry, S. A. (1998) Role of phospholipase D (Pld1p) in growth, secretion, and regulation of membrane lipid synthesis in yeast. *J. Biol. Chem.* **273**, 16635–16638

134. Xie, Z., Fang, M., Rivas, M. P., Faulkner, A. J., Sternweis, P. C., Engebrecht, J., *et al.* (1998) Phospholipase D activity is required for suppression of yeast phosphatidylinositol transfer protein defects. *Proc. Natl. Acad. Sci. U. S. A.* **95**, 12346–12351

135. Rudge, S. A., Sciorra, V. A., Iwamoto, M., Zhou, C., Strahl, T., Morris, A. J., *et al.* (2004) Roles of phosphoinositides and of Spo14p (phospholipase D)-generated phosphatidic acid during yeast sporulation. *Mol. Biol. Cell.* **15**, 207–218

136. Nakanishi, H., Morishita, M., Schwartz, C. L., Coluccio, A., Engebrecht, J., and Neiman, A. M. (2006) Phospholipase D and the SNARE Sso1p are necessary for vesicle fusion during sporulation in yeast. *J. Cell Sci.* **119**, 1406–1415

137. Loewen, C. J. R., Gaspar, M. L., Jesch, S. A., Delon, C., Ktistakis, N. T., Henry, S. A., *et al.* (2004) Phospholipid metabolism regulated by a transcription factor sensing phosphatidic acid. *Science.* **304**, 1644–1647

138. Han, G-S., and Carman, G. M. (2017) Yeast *PAH1*-encoded phosphatidate phosphatase controls the expression of *CHO1*-encoded phosphatidylserine synthase for membrane phospholipid synthesis. *J. Biol. Chem.* **292**, 13230–13242

139. Gaspar, M. L., Aregullin, M. A., Chang, Y. F., Jesch, S. A., and Henry, S. A. (2022) Phosphatidic acid species 34:1 mediates expression of the myo-inositol 3-phosphate synthase gene INO1 for lipid synthesis in yeast. *J. Biol. Chem.* **298**, 102148

140. Hofbauer, H. F., Schopf, F. H., Schleifer, H., Knittelfelder, O. L., Pieber, B., Rechberger, G. N., *et al.* (2014) Regulation of gene expression through a transcriptional repressor that senses acyl-chain length in membrane phospholipids. *Dev. Cell.* **29**, 729–739